BBA - Molecular Basis of Disease 1870 (2024) 166916

Contents lists available at ScienceDirect

BBA - Molecular Basis of Disease

journal homepage: www.elsevier.com/locate/bbadis

AKAP2-anchored protein phosphatase 1 controls prostatic neuroendocrine carcinoma cell migration and invasion

Erica Reggi [a,1], Simon Kaiser [a,1], Nora Sahnane [b], Silvia Uccella [c,d], Stefano La Rosa [b,e], Dario Diviani [a,*]

[a] Department of Biomedical Sciences, Faculty of Biology et Medicine, University of Lausanne, 1011 Lausanne, Switzerland
[b] Unit of Pathology, Department of Oncology, ASST Sette Laghi, Varese, Italy
[c] Department of Biomedical Sciences, Humanitas University, Milan, Italy
[d] Pathology Service, Istituti di Ricovero e Cura a Carattere Scientifico (IRCCS), Humanitas Research Hospital, Milan, Italy
[e] Unit of Pathology, Department of Medicine and Technological Innovation, University of Insubria, Varese, Italy

ARTICLE INFO

Keywords:
A kinase-anchoring protein (AKAP)
Protein kinase A
Protein phosphatase 1
Prostate cancer
Scaffolding proteins

ABSTRACT

Prostate cancer (PC) is the second leading cause of cancer-related death in men. The growth of primary prostate cancer cells relies on circulating androgens and thus the standard therapy for the treatment of localized and advanced PC is the androgen deprivation therapy. Prostatic neuroendocrine carcinoma (PNEC) is an aggressive and highly metastatic subtype of prostate cancer, which displays poor prognosis and high lethality. Most of PNECs develop from prostate adenocarcinoma in response to androgen deprivation therapy, however the mechanisms involved in this transition and in the elevated biological aggressiveness of PNECs are poorly defined. Our current findings indicate that AKAP2 expression is dramatically upregulated in PNECs as compared to non-cancerous prostate tissues. Using a PNEC cell model, we could show that AKAP2 is localized both intracellularly and at the cell periphery where it colocalizes with F-actin. AKAP2 and F-actin interact directly through a newly identified actin-binding domain located on AKAP2. RNAi-mediated silencing of AKAP2 promotes the phosphorylation and deactivation of cofilin, a protein involved in actin turnover. This effect correlates with a significant reduction in cell migration and invasion. Co-immunoprecipitation experiments and proximity ligation assays revealed that AKAP2 forms a complex with the catalytic subunit of protein phosphatase 1 (PP1) in PNECs. Importantly, AKAP2-mediated anchoring of PP1 to the actin cytoskeleton regulates cofilin dephosphorylation and activation, which, in turn, enhances F-actin dynamics and favors migration and invasion. In conclusion, this study identified AKAP2 as an anchoring protein overexpressed in PNECs that controls cancer cell invasive properties by regulating cofilin phosphorylation.

1. Introduction

Prostate cancer (PC) is the second most frequent diagnosed cancer and the 5th most common cause of cancer death in men worldwide [1]. Primary PC mainly relies on circulating androgens to sustain its growth and development. In this context, androgen deprivation therapy, which is the primary treatment for patients suffering from advanced PC, can provide satisfactory clinical control over the disease for some years [2]. Eventually however, PC relapses in the form of a castration resistant prostate cancer (CRPC), which displays invasive and metastatic properties even in the presence of low concentrations of androgens [2].

Prostatic neuroendocrine carcinoma (PNEC) is an aggressive variant of PC, which is characterized by a poorly differentiated neuroendocrine morphology, the absence of androgen receptor expression and the expression of general neuroendocrine markers such as synaptophysin, chromogranin A, and INSM1 [3]. PNEC may arise *de novo* or in patients previously treated with androgen deprivation therapies for prostate adenocarcinoma. Among newly diagnosed PCs, PNECs are relatively rare and represent about 2 % of total cases. This rate can increase up to 17 % in relapsing PCs [4]. The specific molecular determinants driving PNEC cell growth and metastasis are largely unknown with consequent absence of therapies efficiently targeting these processes.

* Corresponding author at: Department of Biomedical Sciences, Rue du Bugnon 27, 1011 Lausanne, Switzerland.
E-mail address: Dario.diviani@unil.ch (D. Diviani).
[1] These authors equally contributed to the work.

https://doi.org/10.1016/j.bbadis.2023.166916
Received 12 June 2023; Received in revised form 20 September 2023; Accepted 6 October 2023
Available online 11 October 2023

Cancer metastasis is a multi-step process that involves cancer cell detachment from the primary tumor [5], acquisition of a mesenchymal phenotype, migration and invasion into the surrounding tissue and blood vessels, and colonization of distal metastatic sites [5,6]. Acquisition of a migratory phenotype is central to the metastatic process and requires a profound reorganization of the actin cytoskeleton of cancer cells [7]. Several studies performed on cultured PC cells have shown that reorganization of actin filaments at the leading edge of migrating cells drives the formation of actin-rich protrusions named lamellipodia and filopodia [8,9]. Lamellipodia generate the driving force for cell movement, whereas filopodia extend from the cell membrane to sense the environment and promote directional movement [10]. Importantly, the kinetics at which these filamentous (F) actin structures polymerize and depolymerize directly influences migration velocity of cancer cells [11,12].

The actin-depolymerizing factor (ADF)/cofilin family members act as central regulators of F-actin dynamics by promoting rapid actin filament severing and disassembly [13]. In particular, cofilin-mediated F-actin severing generates free-barbed ends that are necessary to the addition of new actin monomers and for actin nucleation by the Arp2/3 complex [13,14]. Moreover, cofilin also contribute to the polymerization of new actin filaments by increasing the pool of actin monomers [15]. Cofilin activity is directly regulated by the phosphorylation status of Ser3 near its N-terminus. Phosphorylation of Ser3 by LIM kinases 1 and 2 induces cofilin deactivation whereas dephosphorylation by the Slingshot phosphatases or protein phosphatases 1 and 2A (PP1 and PP2A) promotes cofilin activation [16,17]. Interestingly, it has been shown that active cofilin accelerates actin dynamics and increases migratory and metastatic properties of prostate cancer cells [18]. While these findings highlight a direct link between the cofilin phosphorylation status and PC cell migration, it is currently unknown how cofilin phosphatases and kinases are targeted to the actin cytoskeleton to locally modulate cofilin phosphorylation and activity.

It has become increasingly clear that the subcellular compartmentalization of signaling enzymes controlling the oncogenic properties of cancer cells is regulated by scaffolding and anchoring proteins [6]. In particular, A-kinase anchoring proteins (AKAPs) are scaffold proteins that confer spatiotemporal regulation to signaling events in cells [6,19,20]. AKAPs can assemble a variety of signaling enzymes including the cyclic adenosine monophosphate (cAMP)-dependent protein kinase (PKA), other kinases, phosphatases, phosphodiesterases, adenylyl cyclases, and GTPases, and they can cluster them in proximity of their downstream effector substrates at precise cellular nanocompartments [21–23].

Our current study indicates that AKAP2 is strongly expressed in PNECs as compared to non-cancerous prostate tissues or prostate adenocarcinomas. Using a PNEC cell model and human PNEC tissues, we have demonstrated that AKAP2 forms a signaling complex F-actin and the protein phosphatase 1 (PP1) involved in cofilin dephosphorylation. Accordingly, RNAi-mediated silencing of AKAP2 results in an increase in the phosphorylation status of cofilin and results in a significant decrease in cancer cell migration and invasion. These findings suggest that AKAP2 can control PNEC cell invasive properties by assembling a transduction complex regulating cofilin phosphorylation.

2. Material and methods

2.1. Preparation and immunohistochemical staining of human PNECs

Twelve cases of PNECs, diagnosed on biopsy or trans-urethral specimens at the University Hospital of Varese (ASST Sette Laghi), were included in the study Two cases of non-neoplastic prostatic tissue were included as controls as well. Clinico-pathological information was obtained from patients' clinical records.

The original histopathological slides used for diagnosis were reviewed by two pathologists with expertise in uropathology and endocrine pathology (SLR and SU). Additional slides were cut from significant paraffined inclusions for immunohistochemical and molecular analyses.

To determine AKAP2 expression, deparaffinized sections were immunostained with an affinity purified rabbit polyclonal anti-AKAP2 antibody (custom made, Covance, San Diego, CA, USA) at 1:1000 dilution and a horseradish peroxidase (HRP)-conjugated goat anti-rabbit secondary antibody (GE life sciences, Chicago, IL, USA, 1:500 dilution).

2.2. RNA isolation and quantitative real-time PCR

To determine AKAP2 expression in human PNECs, total RNA was extracted from three paraffinized histological sections after manual microdissection by using Maxwell® RNA FFPE Kit and Maxwell 16 system (Promega, Madison, USA) according to manufacturer's protocol. RNA was quantified using Qubit™ RNA XR Assay Kit (Invitrogen - Thermo Fisher Scientific, Whaltam, USA). Reverse transcription was carried out on 1000 ng of total RNA using High Capacity cDNA Reverse Transcription Kit (Thermo Fisher Scientific, Whaltam, USA) using random primers.

q-PCR reactions were prepared using the reverse-transcribed RNA, AKAP2 TaqMan Gene Expression Assays (Thermofisher scientific, Hs02338795_m1) and TaqMan universal PCR Mastermix (Thermofisher scientific, 4324018). The housekeeping gene Beta-2 microglobulin was used as internal control. q-PCR analysis was performed by using a Quantstudio 6 real-time PCR system (Applied Biosystems).

To determine the expression of AKAP2, synaptophysin and chromogranin A mRNAs expression in LnCAP, PC3 and DU145 PC cells, RNA was extracted from approximately 1 million cells using the RNeasy Mini Kit (QIAGEN, 74106). Single-strand cDNA was synthesized from 500 ng of total RNA by using PrimeScript™ RT Master Mix (Takara, RR036A). q-PCR reactions were prepared using 100 ng of the reverse-transcribed RNA, selected TaqMan Gene Expression Assays (Thermofisher scientific) and TaqMan universal PCR Mastermix (Thermofisher scientific, 4324018). The housekeeping gene GAPDH was used as internal control. q-PCR analysis was performed by using a Quantstudio 6 real-time PCR system (Applied Biosystems).

2.3. Cell culture

HEK-293 cells were cultured in Dulbecco's modified Eagle's medium (DMEM) (Gibco™, 41965-039) supplemented with 10 % fetal bovine serum (FBS) (Gibco™, A5256701) and 100 μg/ml gentamicin (Gibco™, 15750-045). Human prostate cancer DU145, PC3 and LnCAP cells were cultured in Roswell Park Memorial Institute 1640 (RPMI1640) (Gibco™, 61870-010) medium supplemented with 10 % fetal FBS, 5 % GlutaMAX™ non-essential amino acids (Gibco™, 11140-035) and 100 μg/ml gentamicin.

2.4. Plasmids and constructs

AKAP2-003 and AKAP2-003Δ3 splice forms were PCR-amplified from retro-transcribed DU145 cells RNA using the following primers: 5′ TTATAAGCGGCCGCAATGGCGTGGCCCCAGCCCGGG 3′ and 5′ GCGCGCGTCGACTTATTCGTTGTCTTCTTCCTCCTGGTT 3′ and then cloned into the *Not*I and *Sal*I sites in a pEGFP-C1 vector. To generate an AKAP2-003 mutant resistant to siRNA1-mediated silencing, we introduced a silent point mutation in the AKAP2 sequence recognized by the siRNA by site-directed mutagenesis using the following primer: 5′ ACA CGAGTTAACCGCAGGAAG 3′. This AKAP2 silencing resistant construct underwent a second round of site-directed mutagenesis to generate F-actin and PP1 binding deficient mutants (AKAP2-ΔAct and AKAP2-ΔPP1, respectively). For the generation of the AKAP2-ΔAct mutant the following primers were used: 5′ GAT ACT GGG CTA TCC CGA GAA GCG CGA TCA CAT GGT CCT 3′, 5′ TTG CCT GGA ATT CTC CAT CAG CTG AGC TTG TTT AGC AGC AGC AGA AGC ATC TAT 3′. For the generation

of AKAP2-ΔPP1 we used the following primers: 5′ GAT ACT GGG CTA TCC AAC GCG CAA GCA TGA TTG ACA AAG 3′, 5′ CCT GCC AAG CTT GCG TCC GCG AAA CAG CTG TTT CGC GGA CGA AAG CTT GGC AGA 3′. The human cofilin-pcDNA3.1 and human cofilin S3A-pcDNA3.1 constructs were purchased from Addgene (n° 50853 and n°50854). The plasmid encoding the GST fusion of the PP1 binding motif of AKAP2 (residues 716 to 727) was purchased from VectorBuilder Inc. A mutant construct was generated by replacing residues 719, 722 and 724 with alanines.

2.5. SDS-PAGE and Western blotting

PC cells were denaturated in SDS-PAGE sample buffer (4 % SDS, 20 % Glycerol, 100 mM Tris-HCl 0.5 M pH 6.8, 10 % beta-mercaptoethanol) by boiling samples for 5 min at 95 °C and separated on acrylamide gels and electroblotted onto nitrocellulose membrane. Membranes were incubated with primary antibodies and horseradish-conjugated antibodies (Cytiva, NA931-1ML NA934-1ML). The following primary antibodies were used for immunoblotting: anti-cofilin (Cell Signaling Technology, 5175), anti-phospho-cofilin (Ser3) (Cell Signaling Technology, 3311), anti-SSH1 (ECM Biosciences, SP1711) and phospho-SSH1 (Ser-937/978) (ECM Biosciences, SP3901), anti-PP1(Invitrogen, MA5-17240), horseradish peroxidase-conjugated anti-actin (Cell Signaling Technology, 12620), anti-GFP (Sigma Aldrich, G1544), anti-Flag M2 (Sigma Aldrich, F1804) and normal rabbit IgG (Cell Signaling Technology, 2729), anti-PP1CA (Invitrogen, 10C6-3), anti-PP1CC (Santa Cruz, sc-515943). Affinity purified rabbit polyclonal anti-AKAP2 antibodies (Covance, custom made) were described previously [24].

2.6. RNA interference

DU-145 cells were transfected at 80 % confluence with either 30 pmol of control siRNA (Silencer® Select Negative Control No. 1 siRNA, Ambion) or 30 pmol of two AKAP2 specific siRNAs (siRNA1 5′-CACACGGGTTAATCGAAGAAA-3′ and siRNA2 5′CTCCTTACTGATCA CCACGAA-3′) using Lipofectamine RNAiMAX according to the manufacturer's protocol (Thermofisher, 13778075). AKAP2 silencing was evaluated 72 h after transfection.

2.7. Cell invasion assays

Invasion assays have been performed using a modified Boyden Chamber technique measuring the ability of DU145 cells to migrate across an 8 μm pore-size polycarbonate membrane (Corning, 3422) coated with Matrigel basement membrane matrix. DU145 cells were starved in RPMI1640 (Gibco™, 61870-010) containing 0.5 % FBS for 24 h. After trypsinization, 2.5×10^4 quiescent DU145 cells were loaded into the upper chamber. To create a serum gradient across the Matrigel layer, the lower chamber was filled with RPMI1640 supplemented with 10 % FBS. After a 24 h incubation the membrane was fixed in 70 % methanol at −20 °C for 20 min. DU145 that did not migrate were removed and cells migrated on the underside of the membrane were stained using 2 % crystal violet and counted using a light microscope.

2.8. Proliferation assays

1.5×10^5 DU145 cells seeded on 25 mm coverslips and cultured in RPMI1640 supplemented with 5 % non-essential amino acids and 10 % FBS, were transfected with 30 pmol of control or AKAP2 siRNAs. 24 h after transfection, cells were incubated for an additional 24 h in medium with 10 % FBS followed by 1 h incubation with 10 μM BrdU. The concentration of DMSO in the medium was 0.1 % for all experimental conditions. Cells were then washed twice with PBS, fixed for 10 min in PBS/2 % paraformaldehyde, and permeabilized for 20 min with 0.25 % (w/v) Triton X-100 in PBS. Coverslips were incubated for 10 min with ice-cold 1 N HCl, for 10 min with 2 N HCl at room temperature, and for an additional 20 min with 2 N HCl at 37 °C. HCl was then neutralized by two 10 min washes with 0.1 M boric acid (pH 7.5). Coverslips were blocked for 1 h in buffer A (10 mM Tris-HCl [pH 7.5], 155 mM NaCl, 2 mM EGTA, 2 mM $MgCl_2$) supplemented with 1 % BSA. The incorporation of BrdU was assessed by incubating cells for 2 h with a 1:200 dilution of the rat anti-BrdU antibody (Abcam, ab6326) followed by incubation for 1 h with a 1:250 dilution of Alexa Fluor 488-conjugated anti-rat secondary antibodies (Thermofisher, A-21208) and 10 min incubation with DAPI (1 μg/ml). Immunofluorescent staining was visualized using an Advanced Microscopy Group EVOS fluorescence microscope.

2.9. Time-lapse microscopy assay

3×10^4 DU145 cells were seeded in 12 well plates (Corning) in the presence of RPMI1640 containing 10 % FBS. Cells were then transfected either with control or AKAP2 specific siRNAs. Random migration was then visualized 48 h after transfection using a Spinning-disk microscope (Nikon, Eclipse Ti2) over a period of 8 h. Images were taken every 10 min. Cell trajectories and velocities (μm/min) were calculated using the Gradientech Tracking Tool ™ (Gradientech).

2.10. Wound healing assay

3×10^5 DU145 cells were seeded in 6 well plates in the presence of RPMI1640 containing 10 % FBS and transfected either with control or AKAP2 specific siRNAs. 48 h after transfection, confluent monolayers were wounded using a 200 μl tip, washed once with PBS, and cultured for another 36 h in RPMI1640 medium without phenol red. Recolonization of the wounded area was imaged every 6–12 h with an Advanced Microscopy Group EVOS fluorescence microscope. The wounded area was measured using the ImageJ software.

2.11. Proximity ligation assay

DU145 cells seeded on glass coverslips were fixed using 4 % paraformaldehyde for 20 min at 37 °C. Cells were then permeabilized 10 min with 0.1 % Triton-X-100 at 4 °C and coverslips blocked for 1 in PBS supplemented with 1 % bovine serum albumin. Proximity ligation was performed using the Duolink® Proximity Ligation Assay kit (Merck, DUO92008) according to manufacturer's protocol. Primary antibodies against β-actin (Sigma Aldrich, A3853), cofilin (Thermofisher, GT567) and PP1 (Invitrogen, PA5-102349) were used at 1:500 dilution. Cytoskeleton was stained using Actin Green Alexa 488 Ready Probes (ThermoFisher, R37110) and coverslips mounted on microscope slides using DAPI-containing mounting medium. Proximity ligation was also performed on human NEPC sections according to the protocol described by Gomes et al. [25]. In this case, primary antibodies were used at 1:100 dilution.

2.12. AKAP2 and cofilin rescue experiments

DU145 grown in 100 m plates at 80 % confluence were first transfected with 30 pmol of AKAP2 specific siRNA1 using Lipofectamine RNAimax (Thermofisher, 13778075) for 3 h in RPMI1640 without serum. After 2 washes in serum-free RPMI1640, cells underwent a second round of transfection with 16 μg of the silencing resistant mutants of GFP-AKAP2, GFP-AKAP2-ΔAct, and GFP-AKAP2-ΔPP1 or with GFP (2 μg) of cofilin-GFP (6 μg) or cofilin-S3A GFP (6 μg) for 2 h using Lipofectamine 2000 (Invitrogen™, 11668-019). Transfected cells were cultured in RPMI1640 containing 10 % FBS for 48 h, subsequently harvested and used for migration assays or Western blots.

2.13. Peptide arrays

Peptide arrays were synthetized on cellulose membrane using MultiPep spotter at the Peptide array Facility of the University of Oslo. The membranes were then activated in methanol for 30 s. The arrays were blocked 1 h at room temperature in PBS containing 5 % non-fat dried milk followed by incubation with or without 1 μM filamentous actin (Cytoskeleton, APHL99-A). After 3 washes in TBS-Tween, membranes were incubated with horseradish peroxidase-conjugated anti-actin antibodies (Cell Signaling Technology, 12620).

2.14. Immunoprecipitation

DU145 cells seeded in 100 mm petri dishes were lysed in 800 μl of buffer A (50 mM Tris pH 7.4, 150 mM NaCl, 1 % Triton X-100, 0,1 % sodium deoxycholate, 1 μg/ml Leupeptin, Aprotinin and Pepstatin, 0.1 mM PMSF), followed by 2 h incubation at 4 °C on a rotating wheel. Lysates were then centrifuged at 14′000 RPM for 20 min. Supernatants were retrieved and dialyzed twice for 2 h against buffer B (50 mM Tris pH 7.4, 150 mM NaCl, 1 % Triton X-100, 1 μg/ml Leupeptin, Aprotinin and Pepstatin, 0.1 mM PMSF) using Spectra/Por® Biotech Dialysis Membrane (Repligen, 133198). Protein concentration was then assessed using the DC Protein Assay kit (Bio-Rad, 5000112). 2 mg of cell lysates were incubated overnight at 4 °C with 2 μg of rabbit affinity purified anti-AKAP2 antibodies (custom made, Covance) or normal rabbit IgGs followed by 4 h incubation with 30 μl of protein-A-sepharose beads (Thermofisher scientific, 10-1141). Beads were then washed twice for 10 min with buffer C (50 mM Tris pH 7.4, 250 mM NaCl, 1 % Triton X-100, 1 μg/ml Leupeptin, Aprotinin and Pepstatin, 0.1 mM PMSF) and twice with buffer A. Proteins were eluted in SDS-PAGE sample buffer and boiled at 95 °C for 5 min.

2.15. Expression and purification of glutathione-S-transferase (GST) fusion proteins

GST fusions of the WT and mutated PP1 binding motif of AKAP2 were expressed using the bacterial expression vector pGEX4T1 in the Bl21DE3 strain of *Escherichia coli* and purified. To induce the expression of fusion proteins, exponentially growing bacterial cultures were incubated 16 h at 16 °C with 1 mM isopropyl 1-thio-β-d-galactopyranoside (IPTG), and subsequently subjected to centrifugation at 4,000 ×*g* at 4 °C. Pelleted bacteria were lysed in buffer D (20 mM Tris pH 7.4, 150 mM NaCl, 1 % Triton X-100), and protease inhibitors (Thermo Fisher Scientific, catalog n. A32963), sonicated, and centrifuged at 10,000 ×*g* for 30 min at 4 °C. After incubating the supernatants with glutathione Sepharose beads (Cytiva, catalog n°17075601) for 2 h at 4 °C, the resin was washed three times with 10 volumes of buffer C (20 mM Tris pH 7.4, 300 mM NaCl, 1 % Triton X-100, and protease inhibitors). The protein content of the beads was assessed by Coomassie Blue staining of SDS-polyacrylamide gels. Beads were stored at −20 °C.

2.16. GST pulldown experiments

5 μg of GST fusions of the WT and mutated PP1 binding motif of AKAP2 were incubated with 100 nM of purified PP1CB (MyBioSource, MBS965220) in 250 μl of buffer B for 4 h at 4 °C. The beads were then washed twice for 10 min with buffer C and twice with buffer B. Proteins were eluted in SDS-PAGE sample buffer, boiled at 95 °C for 5 min and analyzed by Western blotting.

2.17. Immunocytochemistry

DU145 cells seeded on glass coverslips were fixed with paraformaldehyde 4 % for 20 min at 37 °C. Cells were then washed 3 times in PBS, followed by 2 min permeabilization with 0.1 % Triton X-100 (Sigma). Cells were then blocked using 1 % bovine serum albumin (Roth, 3737.2). Coverslips were incubated overnight at 4 °C with primary antibodies diluted in 0.1 % bovine serum albumin and 2 h with secondary antibodies at room temperature. The following primary and secondary antibodies were used: anti-AKAP2 (Bethyl, A301-363), actinRed 555 Ready Probes (ThermoFisher, R37112), Goat anti-Rabbit IgG (H + L) Secondary Antibody, Alexa Fluor™ 488 (Invitrogen, A11008). Finally, coverslips were mounted on microscope slides using a mounting medium containing DAPI (Roth, HP20.1).

2.18. Statistical analysis

Values are presented as mean ± standard deviation (SD). Statistical differences between two groups were assessed using unpaired 2-tailed Student's *t*-test. 1 or 2-way ANOVA followed by Tuckey tests was used for multiple groups analysis. Values of $p < 0.05$ were considered as statistically significant.

3. Results

3.1. AKAP2 is overexpressed in prostatic neuroendocrine carcinoma

The AKAP2 gene has been reported to be amplified in up to 27 % of PNECs (www.cbioportal.org; Fig. 1A) [26–28] raising the hypothesis that AKAP2 could play a role in coordinating pro-oncogenic responses in this rare but highly metastatic cancer. To address this question, we initially analyzed AKAP2 expression in biopsies obtained from 12 PNEC patients, of whom 8 were affected by *de novo* PNEC and 4 by androgen deprivation therapy-induced PNEC. The mean age of patients was 69.7 years. The histopathological review confirmed the diagnosis of PNEC in all cases, based on the poorly differentiated neuroendocrine morphology and the expression of general neuroendocrine markers (synaptophysin, chromogranin, and INSM1). All cases showed a small cell morphology, being composed of small to medium-sized (2–4 times the size of a small lymphocyte) round to oval cells with scant cytoplasm and hyperchromatic nuclei without nucleoli. Mitotic figures were extremely frequent (>20 mitotes/2mm^2), as well as apoptotic bodies. Ki67 proliferation index was always higher than 60 %. In three cases a residual component of acinar cell carcinoma was also observed.

As shown in Fig. 1B, eleven out of twelve PNEC biopsies displayed increased AKAP2 mRNA levels as compared to non-cancerous prostate tissues. Upregulation was variable and ranged from 2.5 to 520-fold (Fig. 1B). Immunohistochemical analysis of control non-cancerous prostate tissues revealed AKAP2 expression in basal cells of prostatic acini and in vascular pericytes and weak AKAP2 levels in stromal and acinar cells (Fig. 1C, left panels). AKAP2 stainings of biopsies from patients with small-cell PNECs confirmed a significant increase in AKAP2 expression in cancer cells (Fig. 1D, upper panel) whereas no AKAP2 overexpression was detected in prostate adenocarcinomas (Fig. 1D, lower panel). These results suggest that AKAP2 upregulation mainly occurs in PNECs.

To identify human PC cell lines that could represent an *in vitro* model for PNECs, we took advantage of the gene expression atlas provided by NIH Genomic Data Commons (https://gdc.cancer.gov/).This allowed us to select DU145 and PC3 cells as potential candidates based on the observation that they express typical neuroendocrine markers such as synaptophysin and chromogranin A but not androgen receptors. The androgen-dependent PC cells LNCaP, derived from prostate adenocarcinoma cells, were selected as a non-neuroendocrine prostate cancer control cell line. qPCR analysis of synaptophysin and chromogranin A mRNA expression confirmed that DU145 and PC3 cells display 3-to-5-fold increased expression of neuroendocrine markers compared to LNCaP cells (Fig. 1E). In line with our observation that NEPCs but not prostate adenocarcinomas overexpress AKAP2, analysis of AKAP mRNA and protein expression in the three PC cell lines revealed that AKAP2 is selectively expressed in DU145 and PC3 cells but not in LNCaP cells (Fig. 1F–H). As it can be visualized in Fig. 1G, DU145 and PC3 cells

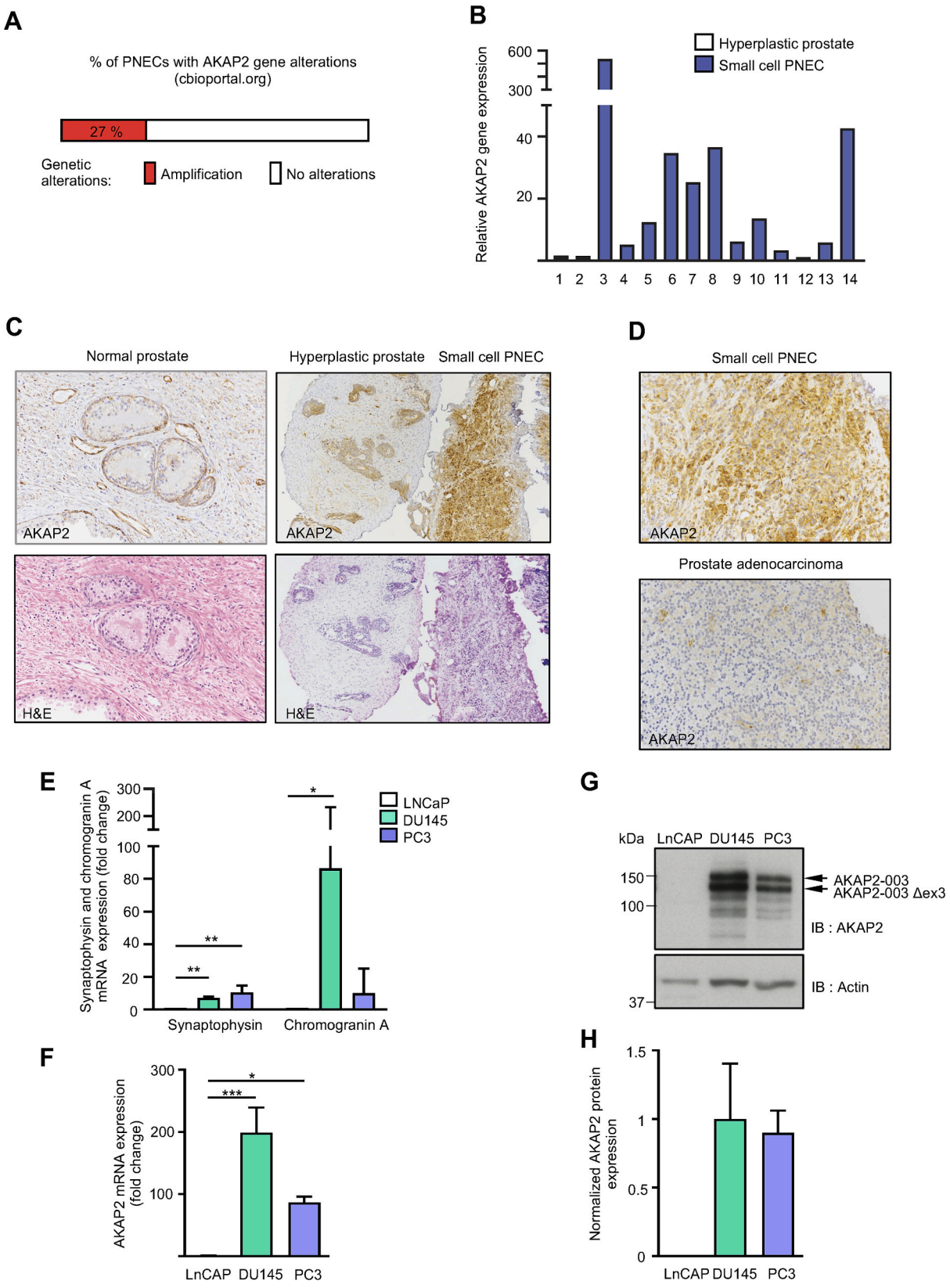

Fig. 1. Neuroendocrine prostate cancers display an increased expression of AKAP2. **A)** % of neuroendocrine prostate cancers displaying amplification of the AKAP2 gene as reported in cBioPortal (https://www.cbioportal.org). **B)** qPCR analysis of AKAP2 mRNA expression in biopsies of control prostates and neuroendocrine prostate cancers. **C)** Anti-AKAP2 (upper panels) and hematoxylin/eosin (lower panels) stainings of sections from human control prostate (left panels) and PNEC (right panels) biopsies. **D)** Anti-AKAP2 stainings of sections of human PNEC (upper panels) and prostate adenocarcinoma (lower panels). **E)** qPCR analysis of synaptophysin and chromogranin A mRNA expression in LnCAP, DU-145, and PC3 prostate cancer cells. Data are expressed as a mean ± SD of 3 independent experiments * $p < 0.05$; ** $p < 0.01$. **F–G)** qPCR (F) and Western blot (G) analysis of AKAP2 expression in LnCAP, DU-145, and PC3 prostate cancer cells. Data are expressed as a mean ± SD of 3 independent experiments * $p < 0.05$; *** $p < 0.001$. **H)** Quantitative analysis of AKAP2 expression in DU-145 cell lysates was obtained by densitometry.

express two main AKAP2 forms. The two forms were PCR-amplified from total DU145 cell RNA and identified as the AKAP2 variant 003 and a variant of AKAP2 003 lacking exon 3 (Fig. S1). Flag-tagged fusion of these AKAP2 proteins displays apparent molecular weights comparable to those of the endogenous AKAP2 forms (Fig. S1).

3.2. AKAP2 mediates DU145 cell migration and invasion

Based on the above results, we initially investigated the possibility that the increased expression of AKAP2 in PNEC cells might confer them increased migratory and invasive potential. To address this question, DU-145 cells were used as a model system for PNECs since they display the highest expression of AKAP2 and neuroendocrine makers (Fig. 1E–H). We initially assessed the impact of AKAP2 silencing on the migratory capacity of DU145 cells using wound-healing assays and single-cell tracking. Results show that knockdown of AKAP2 in DU145 cells using two independent siRNAs (Fig. 2A–B) reduced wound-healing by nearly 50 % (Fig. 2C–D). In line with these findings, migration velocity calculated from single-cell trajectories was also reduced by approximately 40 % (Fig. 2E–H). The involvement of AKAP2 in migration let us to investigate whether a reduction of AKAP2 expression could affect the invasive properties of DU145 cells, assessed by their ability to migrate through a Matrigel layer. As shown in Fig. 2I–L, AKAP2 silencing inhibited DU145 invasion capacity by 50 to 62 %, suggesting that AKAP2 is a key determinant of DU145 cell migration and invasion. Finally, we could show that AKAP2 knockdown does not significantly impact DU145 cell proliferation as determined by monitoring bromodeoxyuridine (BrdU) incorporation (Fig. S2).

3.3. AKAP2 directly interacts with F-actin through a newly identified binding motif

Cell migration is controlled by the reorganization and turnover of the actin cytoskeleton, which provides the driving force for directional movement. Based on our current results linking AKAP2 to DU145 cells migration (Fig. 2), we investigated whether AKAP2 might associate with the actin cytoskeleton. In line with this hypothesis, immunolabeling experiments revealed that AKAP2 is localized both intracellularly and at the periphery of DU145 cells where it exhibits a significant degree of colocalization with F-actin (Fig. 3A). Control experiments indicate that AKAP2 immunostaining is highly specific since it is not detected following RNAi-mediated knockdown of AKAP2 (Fig. 3A). To determine whether AKAP2 and F-actin interact directly and to identify the potential actin binding motif on AKAP2 we used purified F-actin as probe to screen a peptide array of overlapping 20-residue peptides (offset every 3 amino acids) spanning the entire AKAP2 sequence (Fig. 3B). Binding of F-actin was detected using HRP-coupled actin specific antibodies. A major site of interaction was detected between residues 319 and 341 of AKAP2 (Fig. 3B, lower array). In order to delineate specific F-actin binding determinants within this sequence, we generated an array of peptide derivatives where each residue in the binding domain (indicated above the array by single-letter code) was replaced by all 20 amino acids (indicated on the left side of the array) (Fig. 3C). This analysis revealed that the most critical binding determinants within the actin binding site of AKAP2 are represented by arginines at positions 9 and 19 and phenylalanines at positions 5 and 12 (Fig. 3C). In this respect, positions 9 and 10 cannot tolerate residues other than arginines, whereas positions 5 and 12 can accommodate any aromatic amino acid. To determine whether these residues represent the main interacting surface for F-actin on AKAP2, we generated an AKAP2 mutant in which the key arginines and phenylalanines involved in actin binding were substituted by alanines (AKAP2-ΔAct). As shown in Fig. 3D, the ability of immunoprecipitated GFP-tagged AKAP2-ΔAct to bind F-actin in an overlay assay was completely abolished. Altogether, these results suggest that AKAP2 directly interact with F-actin through a newly identified binding motif that requires arginines and phenylalanines.

3.4. AKAP2 regulates cofilin phosphorylation

Our current results indicate that AKAP2 regulates DU145 cell motility and that it directly binds to F-actin (Figs. 2 and 3). Knowing that remodeling of the actin cytoskeleton is main driver of cell migration we investigated the possibility whether AKAP2 could influence the function of known regulators of actin dynamics. To this end, we focused our interest on cofilin since it directly favors actin severing and turnover.

We initially determined whether AKAP2 can affect cofilin phosphorylation state, based on the evidence that the actin-severing activity of cofilin is directly controlled by cofilin phosphorylation at serine 3. Results indicate that AKAP2 silencing in DU145 cells results in a significant 2.3-fold increase in phospho-cofilin levels as assessed by Western blotting using antibodies recognizing phosphoserine 3 (Fig. 4A and B). Conversely, individual overexpression the GFP-tagged AKAP2 003 and AKAP2 003 Δex3 splice variants resulted in a 55 to 83 % decrease in cofilin phosphorylation (Fig. 4C and D). In line with these findings, PLA revealed that AKAP2 and cofilin can form complexes in DU145 cells (Fig. 4E, left panel). Collectively, our findings suggest that AKAP2 interacts *in situ* with cofilin and favors its dephosphorylation.

3.5. AKAP2 anchors PP1 in PNECs

Based on the above results, a possible hypothesis is that AKAP2-medited cofilin dephosphorylation could result from the capacity of this anchoring protein to recruit a protein phosphatase to the actin cytoskeleton in proximity of cofilin. A plausible candidate could be represented by the Slingshot protein phosphatase 1 (SSH1), which has been described as the main regulator of cofilin dephosphorylation [16]. However, co-immunoprecipitation experiments failed to detect an interaction between AKAP2 and SSH1 (Fig. S3A). Similarly, AKAP2 silencing in DU145 cells did not affect the extent of SSH1 phosphorylation on Ser 937 and 978, which is a prerequisite for subsequent SSH1 activation (Fig. S3B and C). This suggests that AKAP2 could regulate cofilin phosphorylation through an SSH1-independent pathway. Accumulating evidence suggests that, in addition to SSH1, protein phosphatase 1 (PP1) can facilitate cofilin dephosphorylation in cancer cells [17,29]. Interestingly, an interaction between AKAP2 and PP1 was identified in DU145 cells when endogenous PP1 was detected in AKAP2 immunoprecipitates (Fig. 5A, upper panel). The ability of AKAP2 to form complexes with PP1 was further confirmed using PLA both in DU145 cells and in sections of primary NEPCs isolated from patients (Fig. 5B and C). As it can be visualized in Fig. 5B and C, complexes could be detected only in samples incubated with both anti-PP1 and anti-AKAP2 antibodies. Interactions between AKAP2 and PP1 were not detected in section from non-cancerous prostates, suggesting that AKAP2-PP1 complexes are mainly formed in NEPC cells (Fig. 5C, lower panels). Interestingly, co-immunoprecipitation experiments performed from PC3 cell lysates did not detect an interaction between AKAP2 and PP1, suggesting that the AKAP2/PP1 complex might not be formed in this PC cell type (Fig. S4).

Analysis of the AKAP2 primary sequence revealed the presence of a potential PP1 interaction site located between residues 709 and 714 and corresponding to the following binding sequence: F-x-x-R/K-x-R/K, where x represents any amino acids (Fig. 5D). To determine whether this site represents the main PP1 binding sequence on AKAP2, we generated an AKAP2 mutant in which the phenylalanine and the two arginines in the putative interacting motif were substituted by alanines (AKAP2 ΔPP1). As shown in Fig. 5E, GFP-AKAP2 but not GFP-AKAP2 ΔPP1 was able to co-immunoprecipitate with the Flag-tagged PP1 catalytic subunit PP1CB, suggesting that AKAP2 interact with PP1 through the predicted motif (Fig. 5E, upper panel). Co-immunoprecipitation experiments failed to detect an interaction between AKAP2 PP1CA and PP1CC suggesting that AKAP2 might preferentially interact with the catalytic subunit PP1CB (Fig. S5). Finally, *in vitro* pulldown experiments performed using a GST-fusion of the PP1CB binding site of AKAP2 and

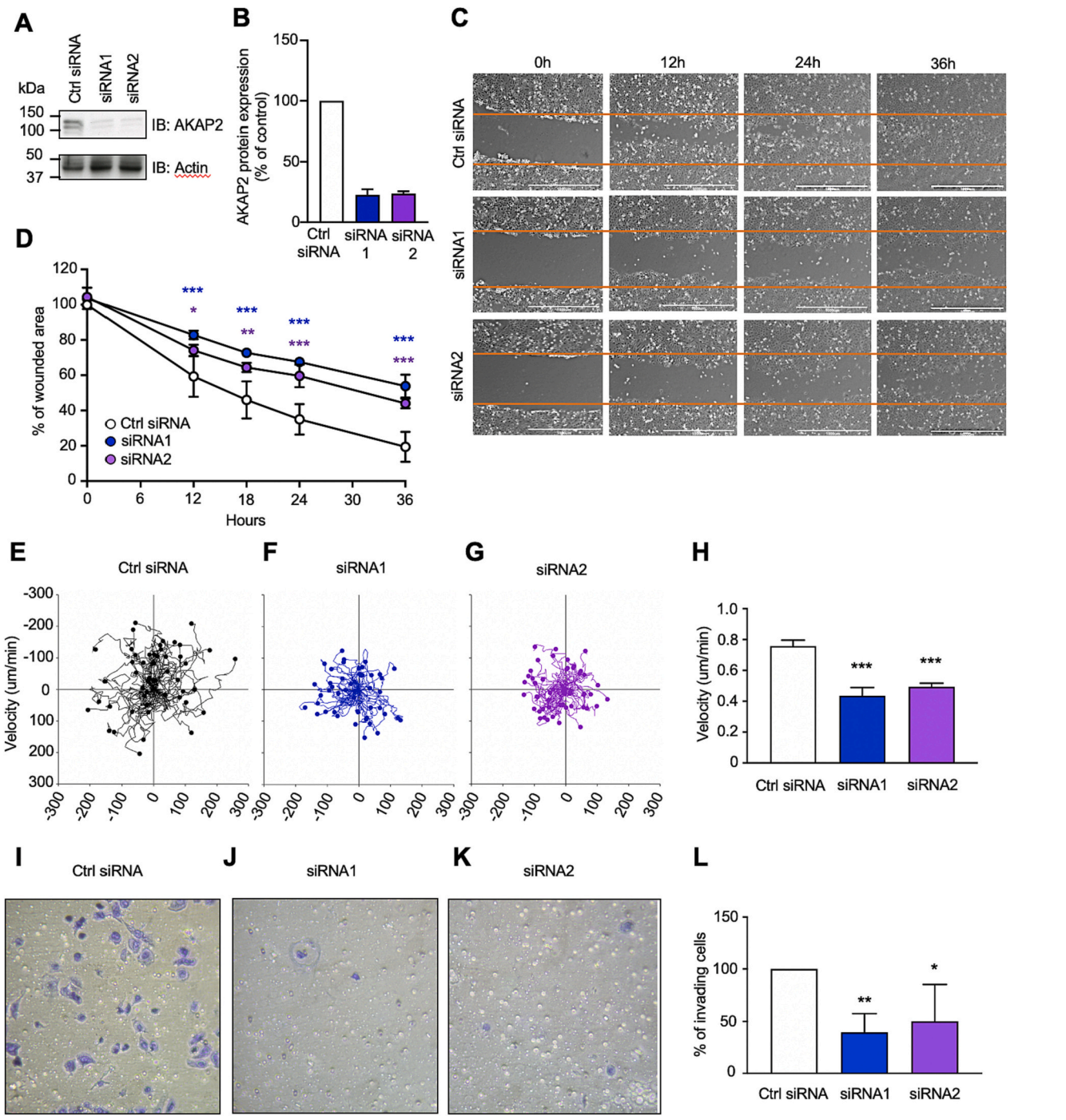

Fig. 2. AKAP2 controls migration and invasion of DU-145 prostate cancer cells. **A)** Western blot analysis of AKAP2 expression in DU-145 cells transfected with control (Ctrl siRNA) or AKAP2 specific siRNAs (siRNA1 and shRNA2). **B)** Quantitative analysis of AKAP2 expression in DU-145 cell lysates was obtained by densitometry. **C)** Wounded DU-145 cell monolayers transfected with Ctrl siRNA, siRNA1 or shRNA2 were cultured for 36 h. Recolonization of the wounded area was imaged every 6–12 h. Scale bar, 1000 μm. **D)** Quantitation of the wound-healing process. $*p < 0.05$, $**p < 0.01$, $***p < 0.001$ compared with the wounded area measured in monolayers transfected with control siRNAs. **E–H)** DU-145 cells were transfected as indicated in A. Random migration was imaged using time-lapse microscopy for 8 h. Migration trajectories (E-G) and velocity (μm/min) (H) were determined on a total of 90 cells per condition. ***p < 0.001 compared with the migration velocity measured in cells transfected with control siRNAs. **I–K)** 2.5×10^4 DU-145 cells transfected as indicated in A, were seeded on Matrigel-coated transwell membranes with 8 μm pores and cultured for 30 h in RPMI1640 supplemented serum. FBS concentration was 0.5 % in the upper chamber and 10 % in the lower chamber. Membranes were fixed and cells that migrated on the underside of the membrane were stained using 2 % crystal violet. Representative fields for each condition are shown. **L)** The percentage of invading cells was determined on three transwell membranes per condition. *p < 0.05, **p < 0.01 compared with the percentage of invading cells measured in cells transfected with control siRNAs.

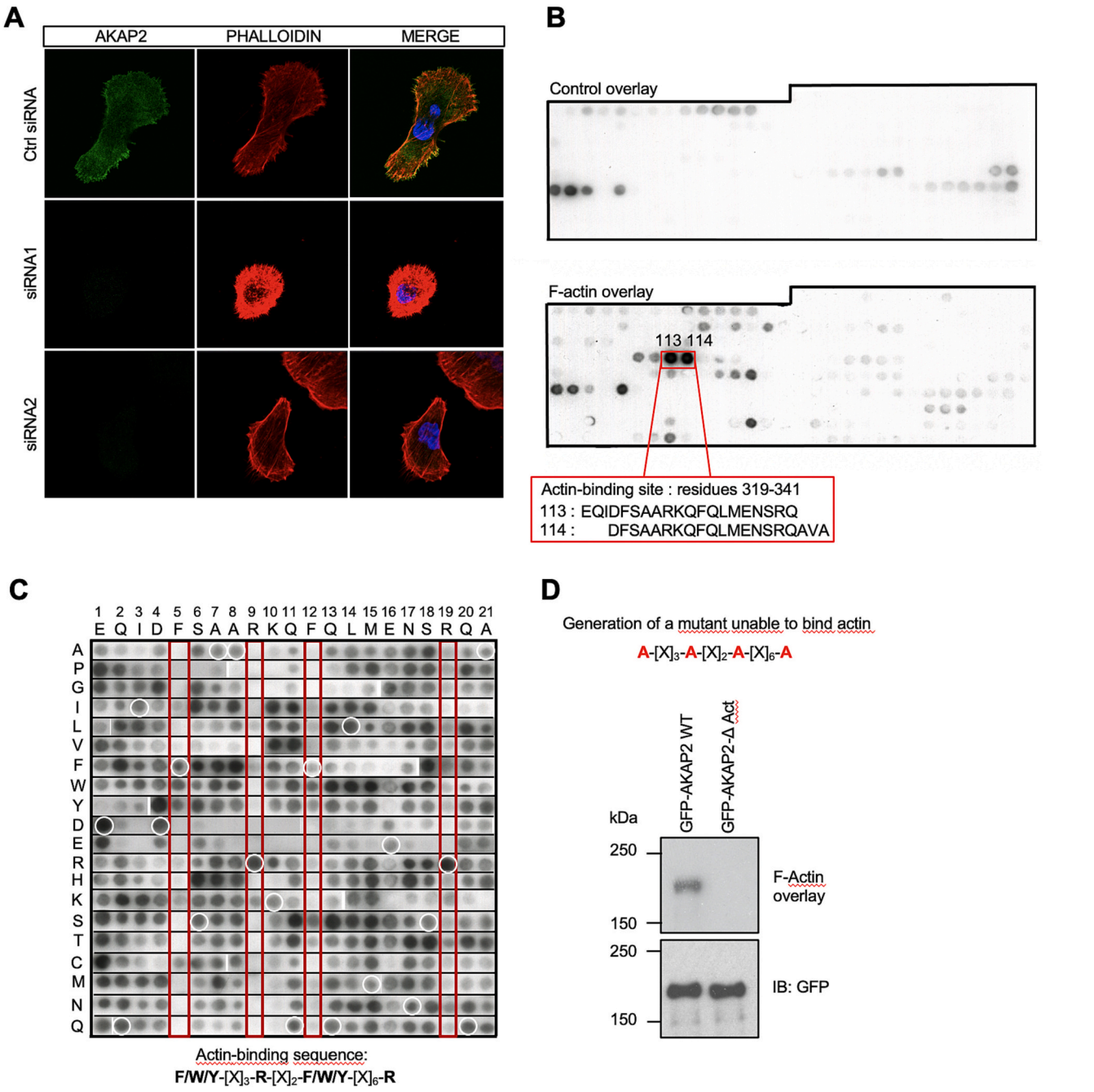

Fig. 3. AKAP2 interacts with actin in DU-145 cells through a newly identified motif. **A)** DU-145 cells were transfected with control (Ctrl siRNA) or AKAP2 specific shRNAs (siRNA1 and shRNA2). 72 h post transfection, cells were fixed and stained. AKAP2 was stained in green using a polyclonal anti-AKAP2 antibody in combination with Alexa Fluor 488 goat anti-rabbit secondary antibody. Actin was detected using Texas red Phalloidin. **B)** Peptide arrays analysis of the F-actin-binding site on AKAP2. Arrays of overlapping 20-amino acid peptides spanning the entire sequence of AKAP2 were incubated with (F-actin array) or without (Control array) 1 μM of F-actin. Solid phase binding was then assessed with HRP-conjugated anti-actin antibodies. The main F-actin binding peptides are numbered and their sequence shown. **C)** Two-dimensional array of AKAP2 peptides where each residue in the F-actin binding sequence (indicated above the array) was replaced with all 20 amino acids (indicated to the left of the array) are shown. F-actin binding was assessed as indicated in A. Replacement of key phenylalanine and arginine resides within the binding motif perturbs F-actin binding (red boxes). Internal control peptides corresponding to the native AKAP2 sequence are indicated by white circles. Below the array, the proposed AKAP2 actin-binding motif, where X represents any amino acids, is shown. **D)** HEK-293 cells were transfected with either GFP-AKAP2 or the GFP-AKAP2-ΔACT mutant in which phenylalanine and arginine resides contributing to F-actin binding were substituted by alanines. 48 h after transfection the AKAP2 constructs were immunoprecipitated from cell lysates using rabbit polyclonal anti-GFP antibodies, separated by SDS-PAGE, and transferred onto nitrocellulose membranes. Membranes were then incubated with F-actin and HRP-conjugated anti-actin antibodies to visualize AKAP2-actin interactions.

purified PP1CB were able to detect an interaction between the two proteins (Fig. S6). In contrast, no binding was detected when pulldown experiments were performed using a mutated PP1binding site (Fig. S6). This suggests that the identified PP1CB-interacting motif directly interacts with the phosphatase.

3.6. AKAP2-anchored PP1 mediates cofilin dephosphorylation

To determine whether anchoring of PP1 to the actin cytoskeleton by AKAP2 controls cofilin dephosphorylation in DU145 cells, we performed experiments that combined knockdown of the endogenous AKAP2 and

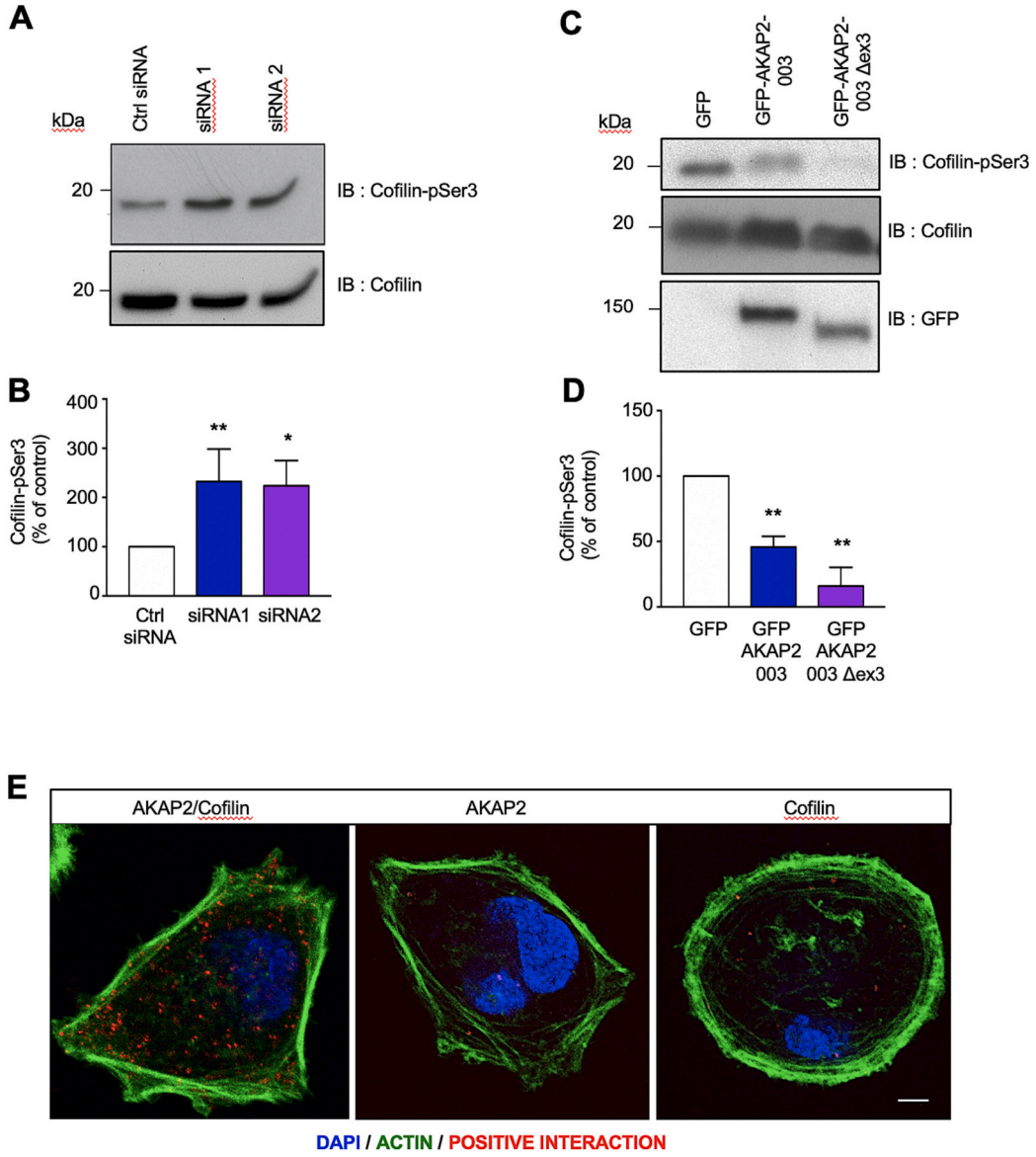

Fig. 4. AKAP2 regulates cofilin phosphorylation state. **A)** DU-145 cells were transfected with a control (Ctrl) siRNA or AKAP2 specific siRNA1 and siRNA2. 72 h after transfection, cell lysates were loaded on SDS-PAGE gels and analyzed by Western blot. Phosphorylated cofilin was detected using antibodies recognizing phospho-serine 3 of cofilin. The amounts of total cofilin were detected using specific antibodies, as indicated. Silencing of AKAP2 was confirmed using an AKAP2 specific antibody. **B)** Quantitative analysis of phosphorylated cofilin was obtained by densitometry. The amount of phospho-cofilin was normalized to the total amount of cofilin. **C)** DU-145 cells were transfected with plasmids encoding either GFP, or two splice forms of GFP-AKAP2 003 that include or miss exon 3 (GFP-AKAP2 003 and GFP-AKAP2 003 Δex3, respectively). 72 h after transfection, the levels of phospho-cofilin, cofilin and GFP constructs in cell lysates were analyzed as indicate in B. **D)** Quantitative analysis of phosphorylated cofilin was performed as indicated in C. Results are presented as the mean ± SD of three independent experiments. * $p < 0.05$; ** $p < 0.01$. **E)** Proximity ligation assay for DU-145 cells incubated with anti-AKAP2 and anti-cofilin antibodies alone or in combination. Nuclei were stained with DAPI and shown in blue whereas F-actin was stained with the Actin Green Ready probe. PLA signals representing positive AKAP2/cofilin interactions are shown in red.

rescue with GFP-tagged wild type and mutant AKAP2 forms that are refractory to siRNA-mediated silencing. Results indicate that rescue with GFP-AKAP2 reduces cofilin phosphorylation back to the levels observed in cells expressing control siRNAs (Fig. 6A, upper panel, Fig. 6B). In contrast, rescue with GFP-AKAP2 ΔAct or GFP-AKAP2 ΔPP1 did not significantly decrease cofilin hyperphosphorylation in silenced cells (Fig. 6A, upper panel, Fig. 6B). AKAP2 silencing and expression AKAP2 constructs was confirmed by Western blot (Fig. 6A). These findings suggest that AKAP2-mediated cofilin dephosphorylation requires the presence of intact actin and PP1 binding domains on the anchoring protein and are consistent with the idea that AKAP2 anchors PP1 to F-actin in proximity of cofilin to facilitate its dephosphorylation.

3.7. AKAP2-anchored PP1 mediates DU145 cell migration

Based on the evidence that cofilin dephosphorylation increases its actin-severing activity and consequently actin turn-over, we investigated whether the AKAP2-PP1 complex regulates DU145 cell migration. To address this question, we evaluated the ability of control, AKAP2 silenced, and rescued cells to migrate using a transwell migration assay (Fig. 6C and D). Results indicate that cell migration is reduced by 55 % following AKAP2 silencing, confirming results shown in Fig. 2. Interestingly, while re-expression of wild type AKAP2 in silenced cells completely rescued their ability to migrate, rescue with the F-actin- or PP1-binding deficient mutants of AKAP2 did not (Fig. 6C and D), suggesting that interactions of AKAP2 with F-actin and PP1 are crucial for

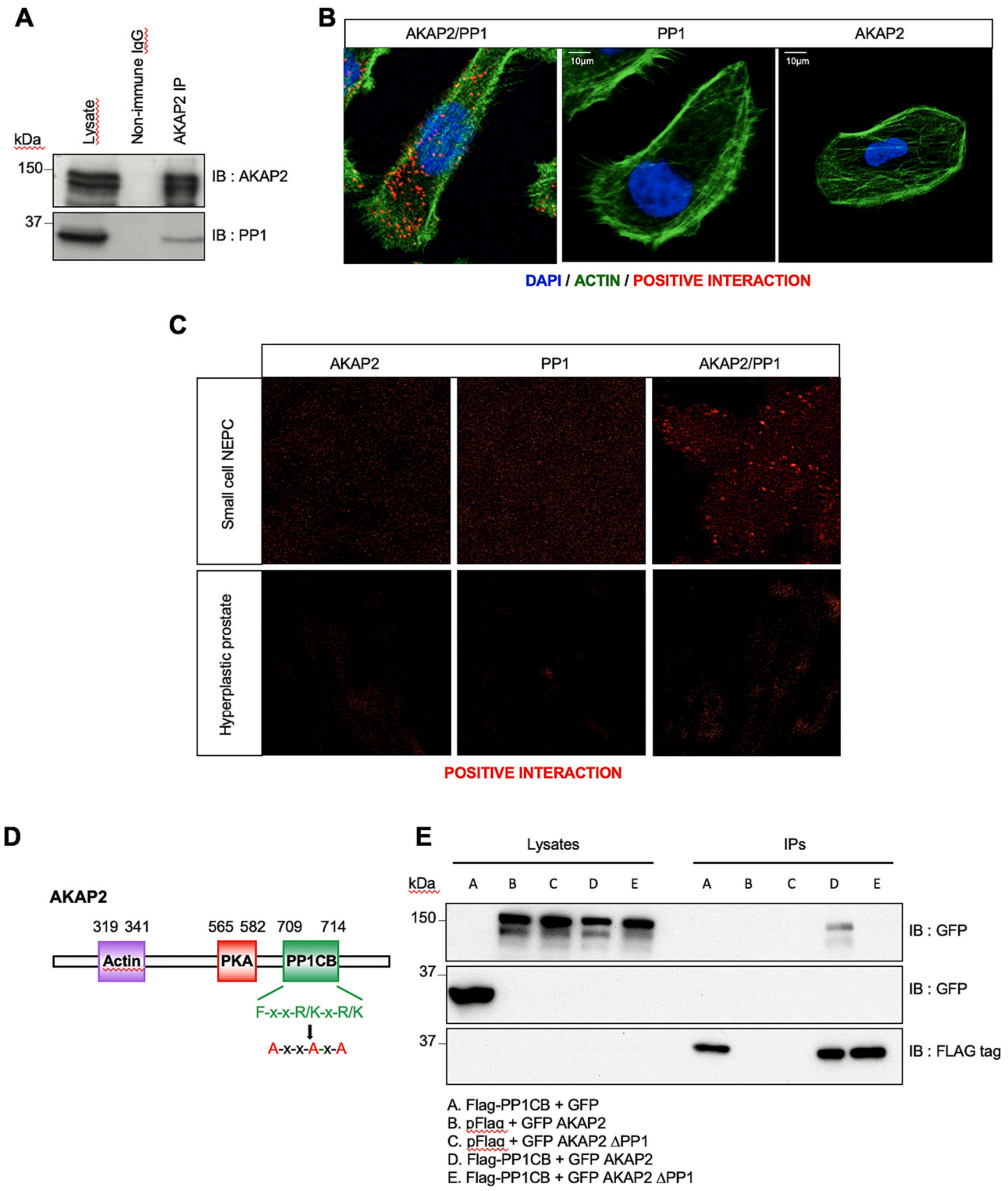

Fig. 5. AKAP2 forms a complex with protein phosphatase 1. **A)** Lysates from DU-145 cells were subjected to immunoprecipitation with either non-immune IgGs or affinity purified anti-AKAP2 antibodies. The presence of PP1 in the lysates and immunoprecipitates was identified by immunoblot using specific antibodies. **B)** Proximity ligation assay for DU-145 cells incubated with anti-AKAP2 and anti-PP1 antibodies alone or in combination. Nuclei were stained with DAPI and shown in blue whereas F-actin was stained with the Actin Green Ready probe. PLA signals representing positive AKAP2/PP1 interactions are shown in red. **C)** Proximity ligation assay for sections of human NEPC biopsies incubated with anti-AKAP2 and anti-PP1 antibodies alone or in combination. Nuclei were stained with DAPI and shown in blue whereas PLA signals representing positive AKAP2/PP1 interactions are shown in red. **D)** Schematic representation and protein domain organization of AKAP2. The actin binding site (residues 319–341), the PKA-binding domain (residues 565–582), and the PP1 interacting motif are shown. Alanine substitutions introduced in the AKAP2 sequence to suppress PP1 binding are indicated in red. **E)** HEK-293 cells were transfected with the empty pFLAG vector or the vector encoding Flag PP1CB in combination with plasmids encoding either GFP, GFP-AKAP2 or the GFP-tagged PP1-binding deficient mutant of AKAP2 (GFP-AKAP2 ΔPP1). Cell lysates were subjected to immunoprecipitation with anti-FLAG antibodies. Western blots of the immunoprecipitates and cell lysates were revealed using rabbit anti-GFP polyclonal antibodies to detect GFP, GFP-AKAP2 or GFP-AKAP2 ΔPP1.

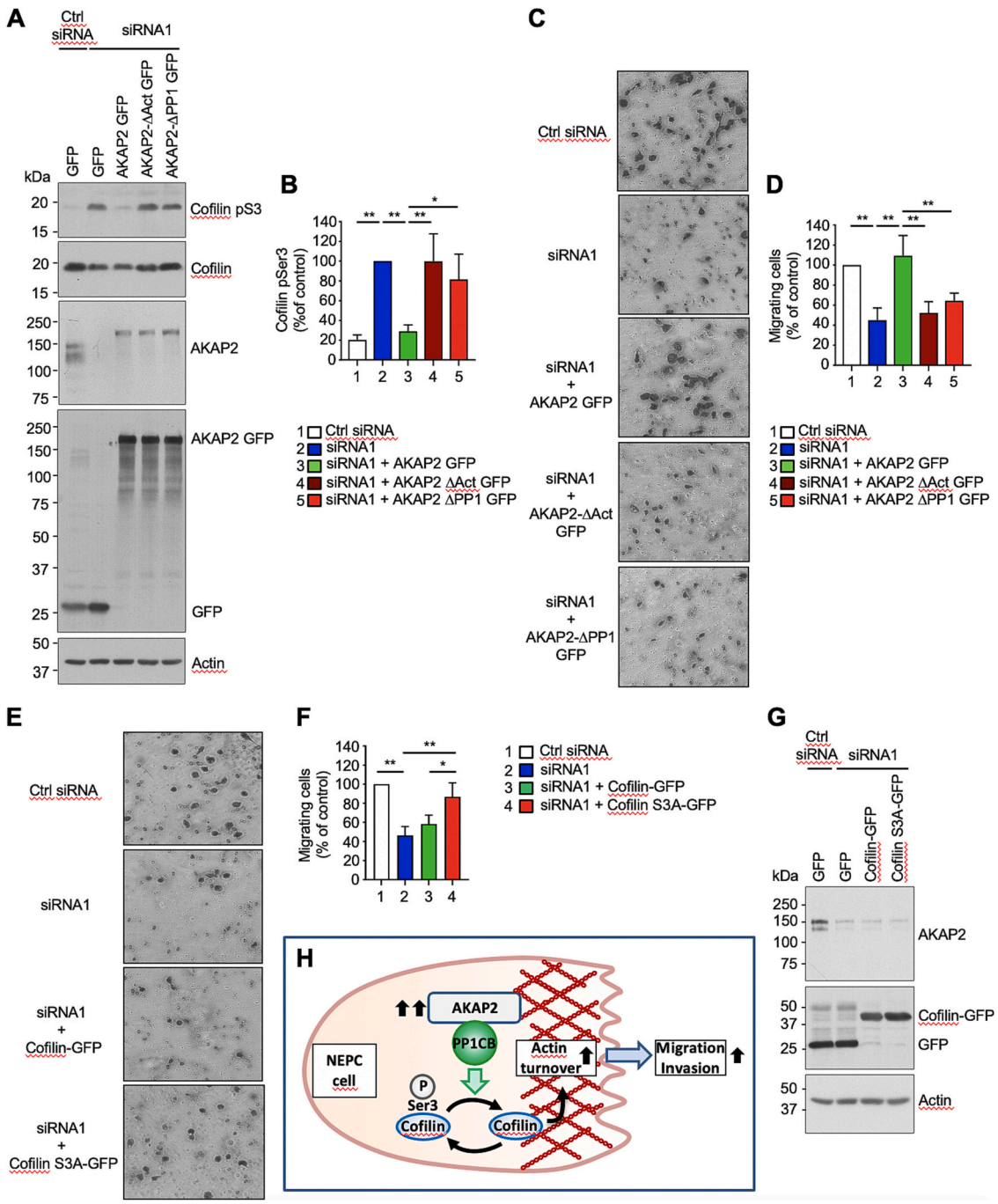

Fig. 6. AKAP2-mediated anchoring of PP1CB to the actin cytoskeleton favors cofilin dephosphorylation and DU145 cell migration. **A)** DU-145 cells were transfected with control (Ctrl) or AKAP2 specific siRNAs (siRNA1) in combination with GFP, AKAP2-GFP or AKAP2-GFP mutants missing the actin-biding domain (AKAP2-ΔAct GFP) or the PP1CB-binsing site (AKAP2-ΔPP1 GFP). 72 h after transfection, cell lysates were loaded on SDS-PAGE gels and analyzed by Western blot. Phospho-cofilin was detected using antibodies recognizing phospho-serine 3 of cofilin. The amounts of cofilin, AKAP2 GFP constructs, and actin were detected using specific antibodies, as indicated. Silencing of AKAP2 was confirmed using an AKAP2 specific antibody. **B)** Quantitative analysis of phosphorylated cofilin was obtained by densitometry. The amount of phospho-cofilin was normalized to the total amount of cofilin. Results are expressed as the mean ± SD of three independent experiments. * $p < 0.05$; ** $p < 0.01$. **C)** DU145 cells transfected as indicated in A) were seeded on transwell membranes with 8 μm pores and cultured for 24 h in RPMI1640 supplemented with 10 % FBS. Membranes were subsequently fixed, and cells migrated on the underside of the membrane were stained using 2 % crystal violet. Representative fields for each condition are shown. **D)** The percentage of migrated cells was determined on three transwell membranes per condition. Results are expressed as the mean ± SD of three independent experiments. * $p < 0.05$; ** $p < 0.01$. E) DU-145 cells were transfected with control (Ctrl) or AKAP2 specific siRNAs (siRNA1) in combination with GFP, cofilin-GFP or a cofilin-GFP phosphorylation-deficient mutant in which serine 3 was mutated into alanine (cofilin S3A-GFP). 72 h after transfection, DU145 cells were seeded on transwell membranes and migration assessed as indicated in C. **F)** The percentage of migrated cells was determined on three transwell membranes per condition. Results are expressed as the mean ± SD of three independent experiments. * $p < 0.05$; ** $p < 0.01$ G) Expression of AKAP2, cofilin-GFP constructs and actin in the lysates was assessed by immunoblot blot using specific antibodies, as indicated. H) Model illustrating the role of the AKAP2/PP1CB signaling complex in mediating migration in PNEC cells. Increased AKAP2 expression favors PP1CB tethering to the actin cytoskeleton, through a direct interaction with F-actin. Anchored PP1CB dephosphorylates Ser3 of cofilin, leading to cofilin activation. This enhances actin turnover, which promotes cell migration and invasion.

DU145 cell migratory capacity.

To provide evidence that the effects of AKAP2 on cell migration are mediated through cofilin, we assessed the impact of expressing wild type or a constitutively active mutant form of cofilin in which serine 3 is substituted by an alanine (Cofilin S3A) in AKAP2 silenced cells [18]. If cofilin acts downstream of AKAP2 to regulate cell migration, then the expression of the cofilin S3A mutant in DU145 cells devoid of AKAP2 should restore their ability to migrate. Our results indicate that while rescue with wild type GFP-tagged cofilin did not significantly enhance migration of AKAP2 silenced cells, re-expression of cofilin S3A-GFP restored DU145 cell migratory capacity (Fig. 6E and F). AKAP2 silencing and expression cofilin constructs was confirmed by Western blot (Fig. 6G). Collectively these findings suggest that the AKAP2/PP1 complex regulates DU145 cell migration through the regulation of cofilin.

4. Discussion

PNEC aggressiveness is linked to its elevated metastatic potential. In this context, understanding how migratory and invasive processes are regulated in PNEC cells would potentially allow the identification of protein targets specifically controlling PNEC metastasis.

In this context, our current findings indicate that AKAP2 expression is strongly increased in PNECs as compared to control prostate tissues (Fig. 1). AKAP2 upregulation appears to be specific to PNECs since it is not observed in prostate adenocarcinomas (Fig. 1). Molecular analysis of the role of AKAP2 in DU145 cells, a prostate cancer cell line expressing neuroendocrine markers, revealed that the anchoring protein assembles a signaling complex that confers increased migratory capacity (Fig. 6H). In particular, AKAP2 recruits PP1CB to the peripheral actin cytoskeleton, where it promotes cofilin dephosphorylation and activation (Fig. 6H). This directly regulates actin turnover, thus favoring cancer cell migration. In line with these findings, AKAP2 silencing in DU145 cells increases cofilin phosphorylation and inhibits migration. Overall, these findings suggest that AKAP2 coordinates a PP1CB based signaling complex coordinating pro-migratory signals at the actin cytoskeleton of NEPCs.

The fact that AKAP2 mRNA and protein expression is strongly upregulated in PNECs but not in prostate adenocarcinomas suggest that transcription of the AKAP2 gene is specifically enhanced during the process of neuroendocrine differentiation. Similarly, AKAP2 expression in PC cell lines highly correlates with the expression of neuroendocrine markers (Fig. 1E–H). Similarly, AKAP2 mRNA expression profiles reported by the NIH Genomic Data Commons (https://gdc.cancer.gov) for various PC cell lines indicate that AKAP2 expression is mainly detected in prostate cancer cell lines expressing neuroendocrine markers (*e.g.* DU145, PC3 and VCAP cells) [30]. Interestingly, analysis of the AKAP2 cistrome using the online platform provided by the Signaling Pathways Project (SPP) (http://www.signalingpathways.org) [31,32], revealed that the promoter region of AKAP2 contains binding sites for transcription factors including N-Myc, Sox2, and Ascl1, and FOXA2 which have been shown to participate in neuroendocrine differentiation of prostate cancers [33–38]. Based on this evidence, one could speculate that upregulation and activation of these transcriptional regulators might increase AKAP2 expression in PNEC cells and consequently enhance their migratory and invasive properties.

In line with our current findings showing that AKAP2 enhances PC motility and invasiveness, recent studies indicate that AKAPs can control migratory and invasive properties in several cancer cell types. In this respect, it has been shown that AKAP13 (AKAP-Lbc) controls the formation of PKA activity gradients that ultimately control migration colon carcinoma cells and promotes RhoA-dependent migration and invasion of PC3 prostate cancer cells [11,39]. Similarly, AKAP220-dependent regulation of GSK3 and IQGAP1 at the leading edge of fibrosarcoma cells influences the polymerization of the actin and microtubule cytoskeleton and, consequently, their migratory properties [40]. On the other hand, recent studies highlight the role for AKAP1 (dAKAP1) in modulating migration and invasiveness of breast cancer cells. In particular, depletion of AKAP1-PKA complexes from the mitochondrial membrane, impaired mitochondrial function, and increases the glycolytic potential and invasiveness [41]. This suggests that AKAPs, by assembling distinct signaling complexes at focal points in cancer cells, can ultimately modulate cytoskeleton dynamics to regulate cancer cell migration and/or invasion.

Previous findings highlighted an association between AKAP2 expression and prostate cancer development. In this regard, silencing of AKAP2 or disruption of the interaction between AKAP2 and PKA has been shown to decrease PC3 prostate cancer cell proliferation and invasiveness. This suggested that AKAP2 regulates PC3 cell oncogenic properties through its interaction with PKA [42]. Surprisingly, this conclusion diverges from our current results, which indicate that AKAP2 silencing does not consistently impact DU145 cell proliferation (Fig. S2). Moreover, co-immunoprecipitation studies performed from DU145 failed to detect regulatory or catalytic subunits of PKA in AKAP2 immunoprecipitates suggesting that AKAP2 does not recruit PKA in this PC cell line (Fig. S7). While the reason of these apparent discrepancies is currently not known, one could speculate that the interaction between AKAP2 and PKA might be regulated by signaling cascades that are differentially activated in DU145 and PC3 cells.

The fact that the AKAP2/PP1 complex is not formed in PC3 cells (Fig. S4) further suggests that AKAP2 assembles profoundly different signaling complexes in DU145 and PC3 cells. In this respect, while DU145 cells rely on the AKAP2/PP1CB signaling complex to transduce promigratory signals, PC3 cells might regulate proliferation and migration through the formation of AKAP2-PKA complexes. The reason why these two cell types use distinct mechanism to regulate cell movement is not clear, but it might be related to the fact PC3 cells might not display the full characteristics of PNECs as shown by the fact that they express lower amounts of chromogranin A compared to DU145 cells (Fig. 1).

Our current findings indicate that the AKAP2/PP1CB signaling complex favors DU145 cell migration by promoting cofilin dephosphorylation. In line with our current results, cofilin activation through dephosphorylation has been shown to promote PC3 prostate cancer cell migration and metastatic spread by enhancing actin severing [18]. Similar observations have been made in breast cancer and colon cancer cells, where cofilin activation generates actin filament barbed ends required for the extension of lamellipodia and migration [43,44]. Interestingly, PC3 cells, similarly to DU145 cells, express AKAP2 and neuroendocrine markers (Fig. 1). This raises the possibility that AKAP2 might selectively favor cofilin activation and increased migratory function in prostate cancer cells undergoing neuroendocrine differentiation.

SSH1 has been shown to act as the main phosphatase involved cofilin dephosphorylation in several cell types [16]. Our present results, however, suggest that AKAP2 favors cofilin dephosphorylation by anchoring PP1CB and not SSH1 (Figs. 5, 6, and S3). Moreover, AKAP2 does not participate in the regulation of SSH1 (Fig. S3). These findings imply that PP1CB functions as a cofilin-phosphatase controlling migratory processes in NEPC cells. In line with this observation, growing evidence suggests that PP1 catalytic subunits play important roles in tumorigenesis by regulating multiple pro-oncogenic pathways promoting cell proliferation and tumor growth, epithelial-mesenchymal transition (EMT) as well as migration and metastasis [45]. In this respect, the PP1CA gene has been found to be amplified in up to 17 % of castration resistant PCs [46], whereas PP1CB has been shown to play pro-migratory and invasive functions by influencing the turnover of focal adhesions [47,48].

Several AKAPs have been shown to anchor PP1 to specific cellular compartments to locally regulate cellular functions. This is the case of AKAP220, which favors PP1-mediated regulation of renal water reabsorption [49] and renal ciliary homeostasis [50]; Yotiao, which targets

PP1 to the *N*-methyl-D-aspartate (NMDA) receptor to regulate channel activity [51]; AKAP149 (D-AKAP1), which regulates nuclear envelope integrity, and AKAP79, which directs PP1 activity towards phospho-PSD-95 [52]. In this context, our current findings that AKAP2-directed targeting of PP1CB enhances PC cell migratory properties further highlight the key role AKAP-mediated PP1 subcellular compartmentalization in specifying the cellular function of this widely expressed phosphatase.

The PP1CB anchoring domain identified on AKAP2 (FKLRSR) conformed to a consensus PP1 binding motif (FxxR/KxR/K) also found in AKAP79 but not to other well characterized PP1 binding sequences including the RVxF, MyPhone, or SILK motifs [52]. Interestingly, in line with the previous observation that the PP1 interacting motif of AKAP79 enhances PP1 activity towards substrates [52], our current findings indicate that deletion of this consensus sequence from AKAP2 increases cofilin phosphorylation. This raises the possibility that anchoring of PP1 through FxxR/KxR/K sequences directs an active pool of the phosphatase in proximity of its downstream targets.

Because PP1 catalytic subunits are abundantly expressed in most tissues and organs, inhibiting their activity does not represent a viable strategy to inhibit PNEC growth and development because of potential widespread toxic effects [53]. Interfering with PP1 subcellular localization by altering the interaction between PP1 anchoring proteins and target sites might offer a more focused approach. However, since the FxxR/KxR/K PP1 binding motif identified on AKAP2 is conserved in other intracellular proteins, one could expect that competitor peptides or small molecules designed to disrupt the interaction between AKAP2 and PP1CB might potentially also interfere with the targeting of the phosphatase to other signaling complexes, and therefore display low specificity. On the other hand, the newly identified actin binding site of AKAP2 is not conserved in other proteins and could therefore serve as basis for the design of cell-permeable competitor peptides that would disrupt the interaction of AKAP2 with F-actin in a more specific manner and consequently inhibit the targeting of PP1CB in proximity of cofilin. In this respect, the F-actin binding sequence of AKAP2 could be fused to cell penetrating cationic peptides to ensure their uptake by PNEC cells [54]. Nevertheless, the *in vivo* success of such an approach might be hampered by an excessive degradation of the peptide by serum proteases. Under these circumstances, one would need to modify the peptide to render it resistant to proteolytic degradation [23].

An alternative strategy could rely on the development of cell-permeable small molecules inhibitors of the AKAP2-F-actin interaction. In this case, the AKAP2-F-actin interaction surface could be targeted by virtual screening of compound libraries. Positive hits would next be tested for their ability to selectively block the interaction [11]. Future experiments will determine whether these strategies can efficiently inhibit PNEC cell migration and invasiveness *in vitro* and *in vivo*.

5. Conclusions

In conclusion, our current findings have several implications. Firstly, they provide evidence that AKAP2 is strongly upregulated in human PNECs where it forms a complex with PP1CB. Secondly, they highlight that the AKAP2-PP1CB signaling complex is targeted to the actin cytoskeleton through a direct interaction with F-actin. Thirdly, they indicate that AKAP2 confers migratory and invasive properties to prostate cancer cells by favoring PP1CB-mediated dephosphorylation and activation of cofilin. This suggests that AKAP2 functions as a signal organizer that enhances cofilin regulation and PNEC cell oncogenic properties.

CRediT authorship contribution statement

Conceptualization, E.R. S.K and D.D.; methodology, E.R., SK.; investigation and data analysis, E.R, N.S., S.K, S.U., S.L, D.D ; writing—original draft preparation, E.R, S.K, D.D.; writing—review and editing, D.D., S.U., N.S., S.L; supervision, D.D.; funding acquisition, D.D.

Ethical approval and consent to participate

Collection and processing of human prostate cancer tissues used for the present study have been carried out in accordance with The Code of Ethics of the World Medical Association (Declaration of Helsinki) for experiments involving humans and was approved by the Ethical Committee of the ASST Sette Laghi, Varese, Italy (prot. nr: 0008465).

Declaration of competing interest

The authors declare that they have no known competing financial interests or personal relationships that could have appeared to influence the work reported in this paper.

Data availability

Data needed to evaluate the conclusions of this study are present in the manuscript and the Supplementary Materials. Further information and requests for reagents may be addressed to, and will be fulfilled by, the corresponding author (D.D.) (dario.diviani@unil.ch).

Acknowledgments

We are grateful to Ivan Gautchi for excellent technical assistance, to Halima Osman for helpful scientific input, and to Marion Delaunay and Simone Spinozzi for critically reviewing the manuscript. This work was supported by grants 31003A_175838 and 310030_212245 of the Swiss National Science Foundation (to D.D).

Appendix A. Supplementary data

Supplementary data to this article can be found online at https://doi.org/10.1016/j.bbadis.2023.166916.

References

[1] World Cancer Research Fund/American Institute for Cancer Research, Diet, Nutrition, Physical Activity and Cancer: a Global Perspective. Continuous Update Project Expert Report. dietandcancerreport.org, 2018.
[2] R.J. Rebello, C. Oing, K.E. Knudsen, S. Loeb, D.C. Johnson, R.E. Reiter, S. Gillessen, T. Van der Kwast, R.G. Bristow, Prostate cancer, Nat Rev Dis Primers 7 (2021) 9, https://doi.org/10.1038/s41572-020-00243-0.
[3] L. Puca, P.J. Vlachostergios, H. Beltran, Neuroendocrine Differentiation in Prostate Cancer: Emerging Biology, Models, and Therapies vol. 9, Cold Spring Harb Perspect Med, 2019, https://doi.org/10.1101/cshperspect.a030593.
[4] Y. Wang, Y. Wang, X. Ci, S.Y.C. Choi, F. Crea, D. Lin, Y. Wang, Molecular events in neuroendocrine prostate cancer development, Nat. Rev. Urol. 18 (2021) 581–596, https://doi.org/10.1038/s41585-021-00490-0.
[5] K. Ganesh, J. Massague, Targeting metastatic cancer, Nat. Med. 27 (2021) 34–44, https://doi.org/10.1038/s41591-020-01195-4.
[6] P.J. Bucko, J.D. Scott, Drugs that regulate local cell signaling: AKAP targeting as a therapeutic option, Annu. Rev. Pharmacol. Toxicol. 61 (2021) 361–379, https://doi.org/10.1146/annurev-pharmtox-022420-112134.
[7] E. Reggi, D. Diviani, The role of A-kinase anchoring proteins in cancer development, Cell. Signal. 40 (2017) 143–155, https://doi.org/10.1016/j.cellsig.2017.09.011.
[8] O.G. Wong, T. Nitkunan, I. Oinuma, C. Zhou, V. Blanc, R.S. Brown, S.R. Bott, J. Nariculam, G. Box, P. Munson, et al., Plexin-B1 mutations in prostate cancer, Proc. Natl. Acad. Sci. U. S. A. 104 (2007) 19040–19045, https://doi.org/10.1073/pnas.0702544104.
[9] Z. Li, Y. Tao, Z. Gao, S. Peng, Y. Lai, K. Li, X. Chen, H. Huang, SYTL2 promotes metastasis of prostate cancer cells by enhancing FSCN1-mediated pseudopodia formation and invasion, J. Transl. Med. 21 (2023) 303, https://doi.org/10.1186/s12967-023-04146-y.
[10] C.D. Lawson, A.J. Ridley, Rho GTPase signaling complexes in cell migration and invasion, J. Cell Biol. 217 (2018) 447–457, https://doi.org/10.1083/jcb.201612069.
[11] D. Diviani, F. Raimondi, C.D. Del Vescovo, E. Dreyer, E. Reggi, H. Osman, L. Ruggieri, C. Gonano, S. Cavin, C.L. Box, et al., Small-molecule protein-protein interaction inhibitor of oncogenic rho signaling, Cell Chem. Biol. 23 (2016) 1135–1146, https://doi.org/10.1016/j.chembiol.2016.07.015.
[12] H. Yamaguchi, J. Condeelis, Regulation of the actin cytoskeleton in cancer cell migration and invasion, Biochim. Biophys. Acta 1773 (2007) 642–652, https://doi.org/10.1016/j.bbamcr.2006.07.001.

[13] G. Kanellos, M.C. Frame, Cellular functions of the ADF/cofilin family at a glance, J. Cell Sci. 129 (2016) 3211–3218, https://doi.org/10.1242/jcs.187849.
[14] S.H. Soderling, Grab your partner with both hands: cytoskeletal remodeling by Arp2/3 signaling, Sci. Signal. 2 (2009) pe5, https://doi.org/10.1126/scisignal.255pe5.
[15] J.J. Bravo-Cordero, M.A. Magalhaes, R.J. Eddy, L. Hodgson, J. Condeelis, Functions of cofilin in cell locomotion and invasion, Nat. Rev. Mol. Cell Biol. 14 (2013) 405–415, https://doi.org/10.1038/nrm3609.
[16] R. Niwa, K. Nagata-Ohashi, M. Takeichi, K. Mizuno, T. Uemura, Control of actin reorganization by slingshot, a family of phosphatases that dephosphorylate ADF/cofilin, Cell 108 (2002) 233–246, https://doi.org/10.1016/s0092-8674(01)00638-9.
[17] K. Mizuno, Signaling mechanisms and functional roles of cofilin phosphorylation and dephosphorylation, Cell. Signal. 25 (2013) 457–469, https://doi.org/10.1016/j.cellsig.2012.11.001.
[18] J. Collazo, B. Zhu, S. Larkin, S.K. Martin, H. Pu, C. Horbinski, S. Koochekpour, N. Kyprianou, Cofilin drives cell-invasive and metastatic responses to TGF-beta in prostate cancer, Cancer Res. 74 (2014) 2362–2373, https://doi.org/10.1158/0008-5472.CAN-13-3058.
[19] M.H. Omar, J.D. Scott, AKAP Signaling Islands: venues for precision pharmacology, Trends Pharmacol. Sci. 41 (2020) 933–946, https://doi.org/10.1016/j.tips.2020.09.007.
[20] J.D. Scott, C.W. Dessauer, K. Tasken, Creating order from chaos: cellular regulation by kinase anchoring, Annu. Rev. Pharmacol. Toxicol. 53 (2013) 187–210, https://doi.org/10.1146/annurev-pharmtox-011112-140204.
[21] A. Murabito, S. Cnudde, E. Hirsch, A. Ghigo, Potential therapeutic applications of AKAP disrupting peptides, Clin. Sci. (Lond.) 134 (2020) 3259–3282, https://doi.org/10.1042/CS20201244.
[22] D. Diviani, J.D. Scott, AKAP signaling complexes at the cytoskeleton, J. Cell Sci. 114 (2001) 1431–1437.
[23] A. Dema, E. Perets, M.S. Schulz, V.A. Deak, E. Klussmann, Pharmacological targeting of AKAP-directed compartmentalized cAMP signalling, Cell. Signal. 27 (2015) 2474–2487, https://doi.org/10.1016/j.cellsig.2015.09.008.
[24] D. Maric, A. Paterek, M. Delaunay, I.P. Lopez, M. Arambasic, D. Diviani, A-kinase anchoring protein 2 promotes protection against myocardial infarction, Cells 10 (2021), https://doi.org/10.3390/cells10112861.
[25] I. Gomes, S. Sierra, L.A. Devi, Detection of receptor heteromerization using in situ proximity ligation assay, Curr. Protoc. Pharmacol. 75 (2016), https://doi.org/10.1002/cpph.15, 2 16 11-12 16 31.
[26] E. Cerami, J. Gao, U. Dogrusoz, B.E. Gross, S.O. Sumer, B.A. Aksoy, A. Jacobsen, C. J. Byrne, M.L. Heuer, E. Larsson, et al., The cBio cancer genomics portal: an open platform for exploring multidimensional cancer genomics data, Cancer Discov. 2 (2012) 401–404, https://doi.org/10.1158/2159-8290.CD-12-0095.
[27] J. Gao, B.A. Aksoy, U. Dogrusoz, G. Dresdner, B. Gross, S.O. Sumer, Y. Sun, A. Jacobsen, R. Sinha, E. Larsson, et al., Integrative analysis of complex cancer genomics and clinical profiles using the cBioPortal, Sci. Signal. 6 (2013) pl1, https://doi.org/10.1126/scisignal.2004088.
[28] H. Beltran, D. Prandi, J.M. Mosquera, M. Benelli, L. Puca, J. Cyrta, C. Marotz, E. Giannopoulou, B.V. Chakravarthi, S. Varambally, et al., Divergent clonal evolution of castration-resistant neuroendocrine prostate cancer, Nat. Med. 22 (2016) 298–305, https://doi.org/10.1038/nm.4045.
[29] A. Ambach, J. Saunus, M. Konstandin, S. Wesselborg, S.C. Meuer, Y. Samstag, The serine phosphatases PP1 and PP2A associate with and activate the actin-binding protein cofilin in human T lymphocytes, Eur. J. Immunol. 30 (2000) 3422–3431, https://doi.org/10.1002/1521-4141(2000012)30:12<3422::AID-IMMU3422>3.0.CO;2-J.
[30] R.L. Grossman, A.P. Heath, V. Ferretti, H.E. Varmus, D.R. Lowy, W.A. Kibbe, L. M. Staudt, Toward a shared vision for cancer genomic data, N. Engl. J. Med. 375 (2016) 1109–1112, https://doi.org/10.1056/NEJMp1607591.
[31] L.B. Becnel, S.A. Ochsner, Y.F. Darlington, A. McOwiti, W.H. Kankanamge, M. Dehart, A. Naumov, N.J. McKenna, Discovering relationships between nuclear receptor signaling pathways, genes, and tissues in Transcriptomine, Sci. Signal. 10 (2017), https://doi.org/10.1126/scisignal.aah6275.
[32] S.A. Ochsner, D. Abraham, K. Martin, W. Ding, A. McOwiti, W. Kankanamge, Z. Wang, K. Andreano, R.A. Hamilton, Y. Chen, et al., The signaling pathways project, an integrated 'omics knowledgebase for mammalian cellular signaling pathways, Sci Data 6 (2019) 252, https://doi.org/10.1038/s41597-019-0193-4.
[33] A. Davies, A. Zoubeidi, L.A. Selth, The epigenetic and transcriptional landscape of neuroendocrine prostate cancer, Endocr. Relat. Cancer 27 (2020) R35–R50, https://doi.org/10.1530/ERC-19-0420.
[34] I. Rapa, M. Volante, C. Migliore, A. Farsetti, A. Berruti, G. Vittorio Scagliotti, S. Giordano, M. Papotti, Human ASH-1 promotes neuroendocrine differentiation in androgen deprivation conditions and interferes with androgen responsiveness in prostate cancer cells, Prostate 73 (2013) 1241–1249, https://doi.org/10.1002/pros.22679.
[35] J.L. Bishop, D. Thaper, S. Vahid, A. Davies, K. Ketola, H. Kuruma, R. Jama, K. M. Nip, A. Angeles, F. Johnson, et al., The master neural transcription factor BRN2 is an androgen receptor-suppressed driver of neuroendocrine differentiation in prostate cancer, Cancer Discov. 7 (2017) 54–71, https://doi.org/10.1158/2159-8290.CD-15-1263.
[36] J.K. Lee, J.W. Phillips, B.A. Smith, J.W. Park, T. Stoyanova, E.F. McCaffrey, R. Baertsch, A. Sokolov, J.G. Meyerowitz, C. Mathis, et al., N-Myc drives neuroendocrine prostate cancer initiated from human prostate epithelial cells, Cancer Cell 29 (2016) 536–547, https://doi.org/10.1016/j.ccell.2016.03.001.
[37] M. Han, F. Li, Y. Zhang, P. Dai, J. He, Y. Li, Y. Zhu, J. Zheng, H. Huang, F. Bai, et al., FOXA2 drives lineage plasticity and KIT pathway activation in neuroendocrine prostate cancer, Cancer Cell 40 (2022), https://doi.org/10.1016/j.ccell.2022.10.011, 1306-1323 e1308.
[38] O.J. Kwon, L. Zhang, D. Jia, L. Xin, Sox2 is necessary for androgen ablation-induced neuroendocrine differentiation from Pten null Sca-1(+) prostate luminal cells, Oncogene 40 (2021) 203–214, https://doi.org/10.1038/s41388-020-01526-2.
[39] A.A. Paulucci-Holthauzen, L.A. Vergara, L.J. Bellot, D. Canton, J.D. Scott, K. L. O'Connor, Spatial distribution of protein kinase A activity during cell migration is mediated by A-kinase anchoring protein AKAP Lbc, J. Biol. Chem. 284 (2009) 5956–5967, https://doi.org/10.1074/jbc.M805606200.
[40] J.S. Logue, J.L. Whiting, B. Tunquist, D.B. Sacks, L.K. Langeberg, L. Wordeman, J. D. Scott, AKAP220 protein organizes signaling elements that impact cell migration, J. Biol. Chem. 286 (2011) 39269–39281, https://doi.org/10.1074/jbc.M111.277756.
[41] S. Aggarwal, L. Gabrovsek, L.K. Langeberg, M. Golkowski, S.E. Ong, F.D. Smith, J. D. Scott, Depletion of dAKAP1-protein kinase A signaling islands from the outer mitochondrial membrane alters breast cancer cell metabolism and motility, J. Biol. Chem. 294 (2019) 3152–3168, https://doi.org/10.1074/jbc.RA118.006741.
[42] A. Thakkar, A. Aljameeli, S. Thomas, G.V. Shah, A-kinase anchoring protein 2 is required for calcitonin-mediated invasion of cancer cells, Endocr. Relat. Cancer 23 (2016) 1–14, https://doi.org/10.1530/ERC-15-0425.
[43] N. Zebda, O. Bernard, M. Bailly, S. Welti, D.S. Lawrence, J.S. Condeelis, Phosphorylation of ADF/cofilin abolishes EGF-induced actin nucleation at the leading edge and subsequent lamellipod extension, J. Cell Biol. 151 (2000) 1119–1128, https://doi.org/10.1083/jcb.151.5.1119.
[44] A. Ferraro, T. Boni, A. Pintzas, EZH2 regulates cofilin activity and colon cancer cell migration by targeting ITGA2 gene, PloS One 9 (2014), e115276, https://doi.org/10.1371/journal.pone.0115276.
[45] J. Felgueiras, C. Jeronimo, M. Fardilha, Protein phosphatase 1 in tumorigenesis: is it worth a closer look? Biochim. Biophys. Acta Rev. Cancer 1874 (2020), 188433 https://doi.org/10.1016/j.bbcan.2020.188433.
[46] M. Chen, L. Wan, J. Zhang, J. Zhang, L. Mendez, J.G. Clohessy, K. Berry, J. Victor, Q. Yin, Y. Zhu, et al., Deregulated PP1alpha phosphatase activity towards MAPK activation is antagonized by a tumor suppressive failsafe mechanism, Nat. Commun. 9 (2018) 159, https://doi.org/10.1038/s41467-017-02272-y.
[47] M. Bianchi, S. De Lucchini, O. Marin, D.L. Turner, S.K. Hanks, E. Villa-Moruzzi, Regulation of FAK Ser-722 phosphorylation and kinase activity by GSK3 and PP1 during cell spreading and migration, Biochem. J. 391 (2005) 359–370, https://doi.org/10.1042/BJ20050282.
[48] J.E. Walsh, M.R. Young, TGF-beta regulation of focal adhesion proteins and motility of premalignant oral lesions via protein phosphatase 1, Anticancer Res 31 (2011) 3159–3164.
[49] J.L. Whiting, L. Ogier, K.A. Forbush, P. Bucko, J. Gopalan, O.M. Seternes, L. K. Langeberg, J.D. Scott, AKAP220 manages apical actin networks that coordinate aquaporin-2 location and renal water reabsorption, Proc. Natl. Acad. Sci. U. S. A. 113 (2016) E4328–E4337, https://doi.org/10.1073/pnas.1607745113.
[50] J. Gopalan, M.H. Omar, A. Roy, N.M. Cruz, J. Falcone, K.N. Jones, K.A. Forbush, J. Himmelfarb, B.S. Freedman, J.D. Scott, Targeting an anchored phosphatase-deacetylase unit restores renal ciliary homeostasis, Elife 10 (2021), https://doi.org/10.7554/eLife.67828.
[51] R.S. Westphal, S.J. Tavalin, J.W. Lin, N.M. Alto, I.D. Fraser, L.K. Langeberg, M. Sheng, J.D. Scott, Regulation of NMDA receptors by an associated phosphatase-kinase signaling complex, Science 285 (1999) 93–96.
[52] A.V. Le, S.J. Tavalin, K.L. Dodge-Kafka, Identification of AKAP79 as a protein phosphatase 1 catalytic binding protein, Biochemistry 50 (2011) 5279–5291, https://doi.org/10.1021/bi200089z.
[53] P.T. Cohen, Protein phosphatase 1—targeted in many directions, J. Cell Sci. 115 (2002) 241–256, https://doi.org/10.1242/jcs.115.2.241.
[54] M.G. Gold, B. Lygren, P. Dokurno, N. Hoshi, G. McConnachie, K. Tasken, C. R. Carlson, J.D. Scott, D. Barford, Molecular basis of AKAP specificity for PKA regulatory subunits, Mol. Cell 24 (2006) 383–395.